



Electronic structure of the corrugated Cu₃N network on Cu(110): Tunneling spectroscopy investigations

K. Bhattacharjee, X.-D. Ma¹, Y.Q. Zhang, M. Przybylski*, J. Kirschner

Max-Planck-Institut für Mikrostrukturphysik, Weinberg 2, 06120 Halle, Germany

ARTICLE INFO

Article history:

Received 14 September 2011

Accepted 7 December 2011

Available online 14 December 2011

Keywords:

Electronic structure

Cu₃N network

Scanning tunneling spectroscopy

ABSTRACT

The local electronic structure of a submonolayer-thick corrugated Cu₃N–Cu(110) network is investigated by low temperature scanning tunneling spectroscopy (LT-STs). The corrugation present in the Cu₃N network plays a vital role by causing the surface electronic features to vary locally due to different N–Cu bonding. Our studies indicate a work function larger by 0.9 eV for Cu₃N compared to bare Cu(110), suggesting the formation of a significant surface dipole. Theoretically predicted various N 2p, Cu 3d hybridized states have been shown and explicitly verified by a combination of constant height and constant current tunneling spectroscopy measurements, thereby providing information about the chemical composition of the N–Cu(110) network.

© 2011 Elsevier B.V. All rights reserved.

1. Introduction

Ultrathin insulating films comprised of alkali halides [1,2], metal oxides [3–5] or metal nitrides [6–10] grown on metal substrates are of considerable technological importance in the miniaturization of microelectronics and magnetoelectronic devices. A reduced charging effect and controlled electronic coupling of such surfaces facilitate the investigation of the local electronic structure of any adsorbed material. Various interesting physical phenomena such as exhibiting single molecule fluorescence [11], atom/molecule charging [12–16], direct imaging of inherent molecular orbitals [1,17] are possible due to such substrate supported ultrathin films. These call for fundamental studies to acquire an improved understanding of the structural and local electronic features of the surface before proceeding towards the physics of the adsorbates. Scanning tunneling microscope (STM), in this regard, with its resolution of imaging and local spectroscopic capabilities at the atomic scale is a versatile tool to probe occupied and unoccupied state features of numerous systems.

Various past and present works demonstrate nitrogen-adsorbed networks of CuN, Cu₂N or Cu₃N on clean Cu single crystals which are only submonolayer (ML) to one ML thick [6–10]. Since adsorbed N on Cu surfaces exhibits ordered [6,7,9,10,18] structures, perfect Cu–N templates are easy to prepare. A large band gap of more than 4 eV of Cu₂N on a Cu(100) surface has been exploited to carry out the spin-flip excitation measurements of single atoms [8], whereas, the

corrugated structure of Cu₃N film on Cu(110) has been used to grow self-organized, epitaxial atomic nanowires of various 3d, 4d and 5d materials [9,19–22]. Despite the fact that N adsorption on Cu surfaces shows a variety of surface nitride phases [23], there are few experimental [24,25] and theoretical [23,24] studies available so far to understand the chemical nature of N/Cu interaction. Among these few studies, most of them are focused mainly on the N/Cu(100) system.

In a recent study, scanning tunneling spectroscopy (STS) investigations on a CuN film grown on a Cu(100) surface showed two unoccupied electronic states at ~2.2 V and ~3.9 V [25]. Although a detailed understanding for the appearance of these two features was not clear, either a CuN conduction band edge, or a Cu(100) surface state, or the out-of-plane N 2p_z state had been considered among the possible reasons for the occurrence of these two states in the STS spectra [25]. Here, we report our systematic results to show the chemical nature of an N-adsorbed corrugated Cu₃N–Cu(110) network by performing low temperature STS (LT-STs) measurements. Moreover, we demonstrate that a combination of two tunneling spectroscopy modes, constant height (CH) and constant current (CC) have been useful to show experimentally various N 2p Cu 3d hybridized states, some of which have been up to now only predicted theoretically [23,24].

2. Experimental details

A Cu(110) single crystal is used to grow a corrugated copper nitride (Cu₃N) molecular network following the procedure as described by Ma et al. [9]. A clean Cu(110) surface is prepared by the usual procedure of Ar⁺ ion sputtering and annealing. To make the Cu₃N network, the clean Cu(110) surface is sputtered with 0.45 keV N⁺ ions at a temperature of 600 K for 1 h, which results in a fully p(2×3)-N reconstructed Cu₃N network. A Cu₃N on Cu(110) surface forms a

* Corresponding author at: Max-Planck-Institut für Mikrostrukturphysik, Weinberg 2, 06120 Halle, Germany. Tel.: +49 345 5582969; fax: +49 345 5511223.

E-mail address: mprzybyl@mpi-halle.de (M. Przybylski).

¹ Present address: Research Center for Advanced Science and Technology, University of Tokyo, 4-6-1 Komaba, Meguro-ku, Tokyo 153-8904, Japan.

polar covalently bonded molecular network with an N coverage of 0.65 ML [9]. The sample preparation and all the measurements are made in an ultrahigh vacuum environment where the base pressure inside the preparation chamber and the STM chamber is maintained at high and low 10^{-11} mbar, respectively. Subsequent STM and STS measurements have been performed with clean W tips at a temperature of 4.7 K. Two different tunneling spectroscopy modes, CH and CC, have been employed to understand the local electronic structure of the Cu_3N network. In the CH mode, after positioning the tip, the STM feedback is turned off to maintain a fixed tip-sample distance during measurement and the tunneling current I is recorded as a function of the voltage V . By adding a 5 mV modulation with a 5.4 kHz frequency, a lock-in amplifier simultaneously measures the differential conductance dI/dV . In the CC mode, the STM feedback loop remains active so that a constant average current is maintained as the gap voltage is ramped from vacuum tunneling through field-emission regimes to give a spectrum of conductance. Tip height $Z(V)$ and the $dI(V)/dV$ from the lock-in (with the modulation parameters the same as mentioned for the CH mode) are simultaneously recorded. The steps in $Z(V)$ show corresponding peaks in $dI(V)/dV$ in the lock-in signal, which signified a change in the local density of states (LDOS) with voltage [25–27].

3. Results

3.1. High resolution STM studies of Cu_3N network

In Fig. 1, we show high resolution constant current STM images of the atomically resolved Cu_3N -Cu(110) network and a schematic

structural model of the same surface. In a previous report, X.-D. Ma and coworkers [9] have investigated a similar system of Cu_3N by STM and by performing *ab-initio* calculations [9]. *Ab-initio* studies performed on this surface suggest a pseudo-(100) atomic reconstruction with a corrugation of the surface Cu layer with two raised and two lowered rows of Cu atoms [9]. Adsorption of N atoms occurs with a regular $c(2 \times 2)$ arrangement at three different hollow sites – top (N_t), middle (N_m) and bottom (N_b); forming a polar covalently bonded Cu_3N molecular network with an N coverage of 0.65 monolayer (ML) [9]. The unit cell of the Cu_3N surface is marked in Fig. 1(a, c) and the positions of the N_t , N_m and N_b atoms in the corrugated network are shown in Fig. 1(b, c). The STM image of the Cu_3N surface [Fig. 1(a)] reveals the distance between two equivalent N atoms along the [001] direction as 11 Å and the distance between two N atoms in each chain along the [1-10] direction as 5 Å which perfectly match with the previous studies [9,23]. This structure corresponds to a Cu_3N network with a $p(2 \times 3)$ -N periodicity [9,23,24] and a corrugation amplitude of ~ 0.5 Å along the [001] direction [9]. The atomic arrangement of the Cu_3N -Cu(110) network can be better understood when looking at the schematic structural model shown in Fig. 1(c).

3.2. LT-scanning tunneling spectroscopy (STS) measurements

3.2.1. Constant height (CH) STS mode

In this section we show the results of CH-STIS studies carried out on a Cu_3N -Cu(110) network. This mode of STIS investigation is particularly important to characterize the electronic structure of the surface around the Fermi level. Fig. 2(a–c) shows the tunneling spectra obtained on Cu(110) and Cu_3N surfaces, whereas Fig. 2(d) shows

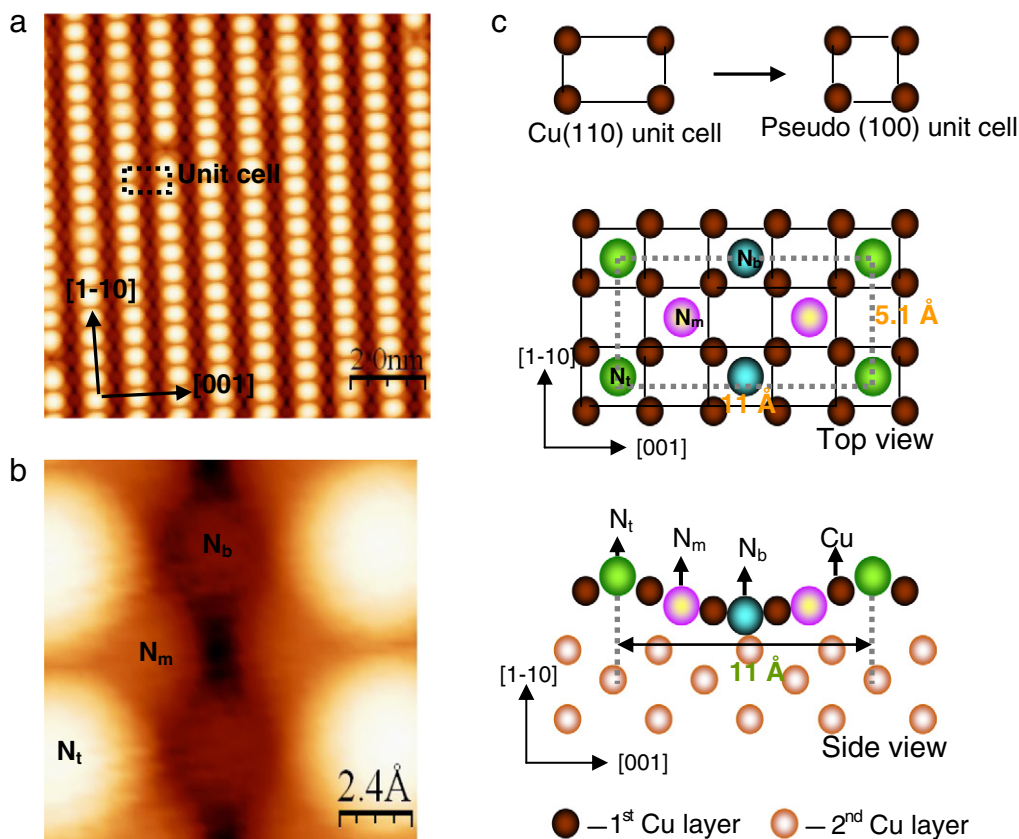


Fig. 1. High resolution STM images of the corrugated Cu_3N -Cu(110) molecular network and the corresponding structural model according to the *ab-initio* calculations given in Ref. [9]. (a) $10 \text{ nm} \times 10 \text{ nm}$ Cu_3N surface. Tunneling parameters – bias voltage V : +0.3 V, current I : 1 nA. The unit cell of the Cu_3N surface is marked in (a). (b) A zoomed-in image of the Cu_3N network ($1.2 \text{ nm} \times 1.1 \text{ nm}$) taken from (a) where the nitrogen top (N_t), nitrogen middle (N_m) and nitrogen bottom (N_b) atom positions within the Cu_3N network are clearly visible. (c) Structural model of the Cu_3N -Cu(110) network. Schematic top view of the $c(2 \times 2)$ periodicity of adsorbed N atoms within a pseudo-(100) surface reconstruction is shown in the upper panel. The (2×3) N unit cell of the Cu_3N -Cu(110) surface with a $11 \text{ Å} \times 5.1 \text{ Å}$ periodicity is marked (dashed lines). The lower panel of the model shows the side view of the corrugated Cu_3N network.

the dI/dV maps of the Cu_3N network at two different biases of +3.4 V and +4.0 V. An overall trend in the tunneling features is shown in Fig. 2(a) comparing bare Cu and a Cu_3N network for a voltage range of -6.0 V to $+4.5$ V. Fig. 2(a) upper panel, shows $I(V)$ characteristics taken on the clean Cu surface and on the Cu_3N -Cu(110) network, whereas Fig. 2(a) lower panel shows the respective dI/dV vs. V spectra acquired from lock-in. An apparent constant current in the $I(V)$ and a corresponding gap in the dI/dV between -4.0 V and $+3.0$ V from both Cu and Cu_3N are due to the choice of a pre-decided higher bias. Such bias was chosen to avoid the lock-in to be overloaded during the measurements while ramping the voltage over the large -6.0 V to $+4.5$ V range. To verify further that the shape of the dI/dV spectra is indeed intrinsic and not due to any artefacts, $I(V)$ data were taken on clean Cu(110) with the same state of the tip but with less extreme set-point parameters. The inset of Fig. 1(a) shows such an $I(V)$ spectrum acquired on Cu(110) for a voltage scan range of -1.0 V to $+1.0$ V. The metallic behavior of Cu is seen in the $I(V)$ curve (inset) with a finite slope around $V=0$. A sudden increase in current in the $I(V)$ [Fig. 2(a), upper panel] beyond ± 4.0 V and a corresponding increase in the dI/dV [Fig. 2(a), lower panel] on bare Cu(110) compared to Cu_3N accounts for an even stronger reduced tunneling barrier with increasing bias on the metal surface than on the nitride surface signifying a higher local surface work-function of the Cu_3N -Cu(110) network compared to Cu(110). Beyond $+3.0$ V, some step-like electronic features are seen in the dI/dV in Fig. 2(a) originating from Cu_3N , whereas

differential conductivity measurements carried out on bare Cu show an exponential increase with bias. To investigate the local electronic features of the corrugated Cu_3N network, a detailed analysis is performed in two ranges of the bias voltage. Fig. 2(b) shows the $dI(V)/dV$ spectra from Cu_3N and from bare Cu for a voltage range of -1.5 V to $+2.5$ V, whereas Fig. 2(c) shows similar differential conductivity curves acquired from the Cu_3N surface for a bias voltage of $+2.5$ V to $+4.5$ V. Compared to Cu(110), the Cu_3N surface shows a reduced differential conductivity [Fig. 2(b)] in the positive voltage up to approximately $+1.7$ V beyond which an, exponential dependence of the tunneling signal with bias is observed. No sharp, distinct peak feature in the STS spectra is seen in this set of measurements carried out for a voltage range scan of -1.5 V to $+2.5$ V [Fig. 2(b)]. However, precise atom specific tunneling spectroscopy measurements performed on top of the N_t , N_m or N_b atom of the corrugated Cu_3N network show a variation in the $dI(V)/dV$ signal for different atoms [Fig. 2(b)]. A broad electronic feature from the Cu_3N network is observed in the CH STS spectra in Fig. 2(b) which extends and crosses the Fermi level (E_F). The intensity of this feature varies, where N_t atoms show a higher dI/dV signal compared to N_m and N_b atoms. To further check the step-like features [Fig. 2(a)] on the corrugated Cu_3N network beyond $+3.0$ V, the tunneling spectra starting from $+2.5$ V to $+4.5$ V [Fig. 2(c)] are examined. In this range, one can see [Fig. 2(c)] shoulder-like unoccupied electronic features appearing in the $dI(V)/dV$ spectra from the Cu_3N surface at around $+3.4$ V and $+4.0$ V. This feature is more prominent from the N_t

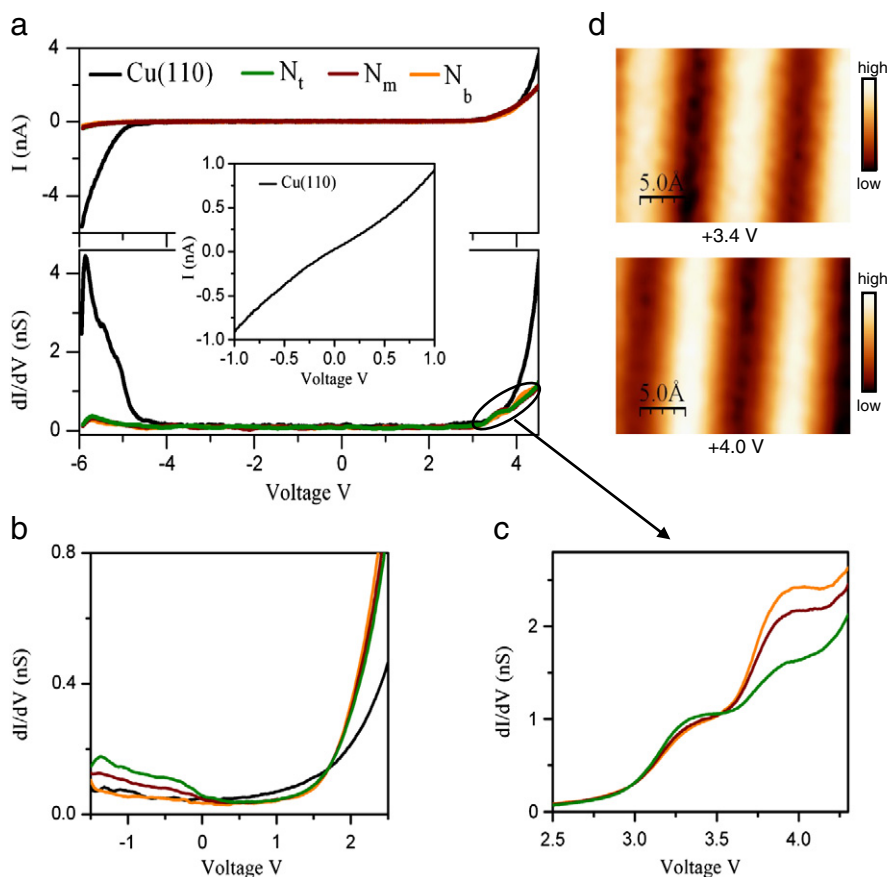


Fig. 2. CH tunneling spectroscopy measurements on corrugated Cu_3N network (a, b, c) and dI/dV maps of the Cu_3N surface (d). The tunneling parameters to acquire the set of data in (a) and (c) – bias voltage, V : $+4.0$ V and initial tunneling current I : 1 nA and for (b) $+2.0$ V and 1 nA respectively. Inset of (a) shows an $I(V)$ curve [V : $+1.0$ V, initial I : 1 nA] acquired on a bare Cu(110) surface with the same tip condition. A finite slope of $I(V)$ at $V=0$ is observed on Cu as a confirmation of its metallic behavior. Shoulder-like features appear in the STS spectra at $+3.4$ V and $+4.0$ V from nitrogen top (N_t), nitrogen middle (N_m) and nitrogen bottom (N_b) atoms of the Cu_3N network as seen in (a) and (c). The feature at $+3.4$ V is dominated by N_t atoms, whereas the feature at $+4.0$ V is dominated by N_b atoms. (d) dI/dV maps (2.5 nm \times 1.9 nm) of the Cu_3N surface at $+3.4$ V and $+4.0$ V. The crest regions in the dI/dV image taken at $+3.4$ V appear as troughs at $+4.0$ V and vice versa. Difference in the local electronic structure of the Cu_3N network is clearly evident where tunneling is dominated via different local density of states at two different biases of $+3.4$ V and $+4.0$ V.

atoms compared to N_m and N_b atoms at +3.4 V, whereas an opposite trend is observed for the features at +4.0 V. In Fig. 2(d), the dI/dV images of the Cu_3N network are shown for +3.4 V and +4.0 V, respectively. In the dI/dV images, a reversal of the contrast between N_t and N_b atoms with respect to the bias value is observed. The N_t atoms, which appear as bright protrusions at +3.4 V, appear dark at +4.0 V and vice versa. The tunneling spectroscopy measurements [Fig. 2(a–c)] carried out on top of the N_t , N_m and N_b atoms of the corrugated Cu_3N –Cu(110) network match with the energy mappings [Fig. 2(d)] of the surface as shown here. However, the CH-STs measurement has its own limitations due to the setting up of an initial tip-sample separation where the set bias voltage is comparable to the highest bias value to be ramped during measurements. In addition, this mode of STs is difficult to apply in order to find out the work function of the surface or to probe the image potential states in front of the metal surfaces.

3.2.2. Constant current (CC) STS mode

In order to achieve spectroscopic information over a wide voltage range, CC tunneling spectroscopy measurements have been performed with a varying tip-sample distance keeping the feedback loop on. In Figs. 3 and 4 we present CC-STs studies carried out on top of N_t , N_m and N_b atoms of a Cu_3N network and on a bare Cu(110) surface for both positive and negative biases. The change of tip height (Z) with bias (V) on bare Cu and on N_t , N_m and N_b atoms of the corrugated nitride network is shown in Fig. 3(a) and in Fig. 4(a). The $Z(V)$ [Figs. 3(a), 4(a)] spectra are given a vertical shift for better clarity. Data from 0 to +0.5 V [Fig. 3(a, b)] and 0 to –0.8 V [Fig. 4(a, b)] are omitted due to the divergence of the dI/dV signal with approach towards zero bias. Peaks at +3.4 V and +4.0 V in the CC-STs spectra [Fig. 3(b)] show intensity dependence of the probed atoms (N_t , N_m and N_b) of the Cu_3N network exactly in the same way as it was observed in the CH-STs measurements [Fig. 2(c)]. However, in the CC-STs studies, we observe an additional feature at +2.0 V which was not evident in the CH-STs studies, most likely due to the large dI/dV at +2.0 V at the sample-tip distance chosen in this

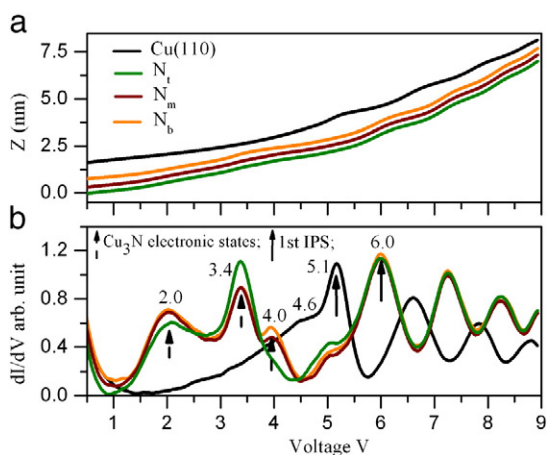


Fig. 3. CC-STs measurements on corrugated Cu_3N network and on a bare Cu(110) surface. All spectra are acquired at an initial tunneling condition of $I: 1$ nA, $V: +0.2$ V. Data from +0.2 V to +0.5 V (a, b) are omitted to avoid the artifacts at around $V=0$ due to a closed feedback loop. Tip height (Z) vs. voltage (V) (a) and the respective differential conductivity curves (b) from Cu and Cu_3N surfaces are plotted covering a voltage range of +0.5 V to +9.0 V. In (a), each of the $Z(V)$ curves has been given a vertical shift for better clarity. (b) In the unoccupied states, Cu_3N network shows 3 additional peaks compared to the Cu(110) surface in the vacuum tunneling regime at +2.0 V, +3.4 V and +4.0 V (these peaks are identified with dashed arrows). In addition, a series of pronounced peaks starting from +5.1 V and +6.0 V from Cu and Cu_3N surfaces, respectively, in the field emission regime are the IPS (these peaks are marked as continuous arrows).

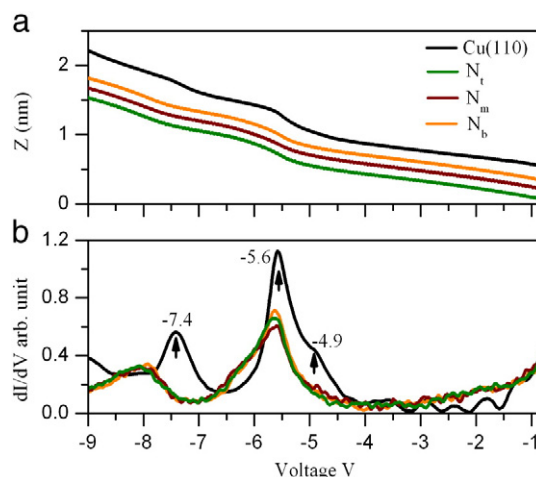


Fig. 4. CC-STs measurements on a corrugated Cu_3N network and on a bare Cu(110) surface. All spectra are acquired at a tunneling condition of $I: 1$ nA, $V: -0.2$ V. Data from –0.2 V to –0.8 V (a, b) are omitted to avoid the artifacts at around $V=0$ due to a closed feedback loop. Tip height (Z) vs. voltage (V) (a) and the respective differential conductivity curves (b) from the Cu and Cu_3N surfaces are plotted covering a voltage range of –0.8 V to –9.0 V. Each of the $Z(V)$ curves in (a) is vertically shifted for better clarity. (b) Occupied electronic states show a shoulder-like feature at –4.9 V and pronounced peak at –5.6 V, which we attribute to Cu 3d states, whereas the peak at –7.4 V is attributed to Cu 4s state features at –5.6 V and –8.0 V in the STs spectra from the Cu_3N surface are due to the N 2p and Cu 3d hybridized electronic states.

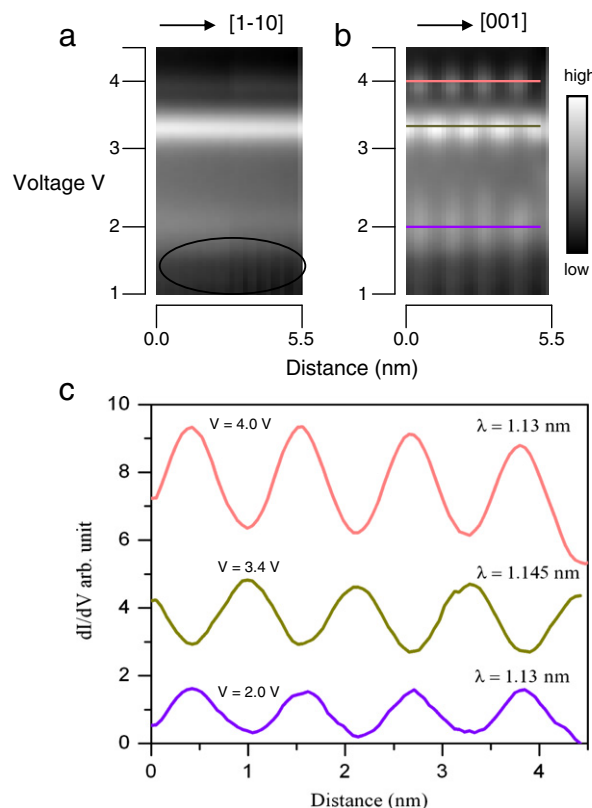


Fig. 5. Differential conductivity, dI/dV (in black and gray scale) against the bias voltage, V (Y axis) and the position (X axis) measured on the straight lines along (a) [1–10] and (b) [001] directions. These plots result from 128 dI/dV vs. V curves taken along lines with each point positioned 0.43 \AA apart. Two strong electronic modulations are observed in (a) at biases of 2.0 V and 3.4 V and one extra modulation is observed in (b) at a bias of 4.0 V. Modulations in (a) do not exhibit any strong electronic oscillation of any particular periodicity, though, sometimes a weak periodic oscillation with a periodicity of 0.51 nm is observed within the modulation at 2.0 V. However, very strong oscillations are observed in (b) within the modulations at biases of 2.0 V, 3.4 V and 4.0 V. In (c), dI/dV profiles are plotted along the lines shown in (b). These oscillations correspond to a periodicity (λ) of 1.13 nm (at 2.0 V), 1.145 nm (at 3.4 V) and 1.13 nm (at 4.0 V).

mode. Unoccupied states of the Cu_3N surface [Fig. 3(b)] show two peak features originating from N_t atoms, the first peak or a shoulder kind of feature appears at around +2.0 V and the second one, a sharp feature, appears at +3.4 V. Three unoccupied electronic states are observed in the tunneling spectra from N_m and N_b atoms of the Cu_3N network at around +2.0 V, +3.4 V and +4.0 V. The peak at +4.0 V appears more prominent for N_b atoms than for N_m atoms. All these peaks which appear in the CC-STs spectra below +4.5 V are associated with the Cu_3N -Cu(110) network and are not the characteristic features of the Cu(110) [Fig. 3(b)].

When STS measurements are performed in the CC mode at higher bias voltages in a transition region between tunneling and field emission, a series of sharp resonances are available due to enhanced tunneling. In Fig. 3(b), the clean Cu(110) surface exhibits such sharp, narrow peaks starting from +5.1 V in the STS spectrum, whereas no peak-like feature is observed below +5.1 V for Cu(110). Such sharp states are also observed on the corrugated Cu_3N surface. However, peaks at +5.1 V or above have moved toward higher energy by 0.9 V with respect to Cu(110) [Fig. 3(b)]. The first peak from the Cu_3N surface is observed at around +6.0 V for the same tunneling conditions as mentioned for the Cu(110) surface. The shoulder-like feature which was observed at +4.6 V for Cu is now shifted to +5.0 V for the Cu_3N surface.

In the negative bias range [Fig. 4(a, b)], we observe an onset at -4.9 V and two pronounced peak features at -5.6 V and at -7.4 V in the STS spectrum from Cu(110) as shown in Fig. 4(b). Similar peaks at -5.6 V are also observed from N_t , N_m and N_b atoms of the Cu_3N film in the STS spectra, however, the feature at -7.4 V which was observed on clean Cu(110) is missing at the Cu_3N surface, whereas an additional peak appears at Cu_3N at around -8.0 V.

Fig. 5 shows spatially resolved (SR) STS maps of the corrugated Cu_3N network taken along the lines parallel to [1-10] [Fig. 5(a)] and [001] [Fig. 5(b)], respectively, in CC mode. Each data point was chosen 0.43 Å apart on the lines, feedback loop closed, to maintain CC during the dI/dV measurements. The line along [1-10] was chosen on top of the N_t atoms of the corrugated network. By plotting the differential conductance dI/dV as a function of the voltage (V) and the position (r), we can see two strong electronic modulations appearing at bias voltages of +2.0 V and +3.4 V along [1-10] [Fig. 5(a)], whereas a series of three electronic modulations are observed along [001] at bias voltages of +2.0 V, +3.4 V and at +4.0 V [Fig. 5(b)], respectively. The intensity of the modulation at +2.0 V appears less in both cases compared to the modulation at +3.4 V in agreement with the STS results [Fig. 3(b)]. The other features to be noted here are that the modulations at +2.0 V and +3.4 V along [1-10] do not exhibit any strong periodic oscillations within them [Fig. 5(a)]. However, a weakly visible oscillation with a periodicity (λ) of 0.5 nm is observed within the modulation at +2.0 V along [1-10] as shown and marked in Fig. 5(a). In contrast to the modulations along [1-10], each of the modulation along [001] [Fig. 5(b)] shows clear and distinct periodic oscillations. In Fig. 5(c), we plot the dI/dV profiles taken along the lines marked in Fig. 5(b).

4. Discussion

In order to understand the possible physical origin of the occupied and unoccupied electronic states as observed in the STS spectra of the Cu_3N -Cu(110) network, we have attempted to look into how the Cu DOS is modified by the adsorption of N. The surface nitride structure of Cu_3N involves a pseudo-(100) reconstructed surface layer of Cu(110) with a $c(2 \times 2)$ adsorption of N atoms which is similar to that observed for N chemisorption on Cu(110) [9]. The full-potential linear muffin-tin orbital (FP-LMTO) calculations carried out on atomic N adsorbed on Cu(100) show the hybridization between N 2p and Cu 3d states where the out-of-plane N 2p_z states were separated from the in-plane 2p_{xy} states [24]. According to the calculations, the N

2p_z orbitals interact strongest with 3d orbitals of the 1st and 2nd Cu layers and a little with the 4s orbitals of the Cu 2nd layer. The N 2p_{xy} orbitals strongly couple to the 3d and 4s orbitals of the 1st layer Cu [24]. In addition, the first-principles density functional theory (DFT) calculations [23] performed on N/Cu(110) show that the N 2p Cu 3d bonding states extend from -8 to -4 eV, antibonding states extend from -2 to 2 eV with Cu 3d nonbonding states in between.

With all this information, a qualitative understanding is developed towards the local electronic features appearing in the STS spectra from the pseudo-(100) Cu_3N -Cu(110) network [9]. In Fig. 6, we present a schematic energy level diagram summarizing all the N 2p-Cu 3d hybridized electronic state features appearing in the STS spectra from an N adsorbed Cu(110) surface (as reported in Subsection 3.2 "LT-Scanning Tunneling Spectroscopy (STS) measurements").

To discuss the unoccupied state features in the STS spectra [Figs. 2(a-c), 3(b)] originating from the Cu_3N -Cu(110) network, the peak at +2.0 V [Fig. 3(b)] could be due either to a hybridized electronic state at the Cu_3N /Cu(110) interface derived from a Cu(110) surface state at ~2.0 V above the Fermi level [28,29], or to an antibonding state between the adsorbate 2p orbital and Cu 3d orbital as shown in DFT calculations on N/Cu(110) [23]. It could also be that this peak is due to the conduction band edge of the Cu_3N -Cu(110) surface as discussed in ref.[25] for CuN film on Cu(100). The feature at +3.4 V in the STS spectra [Fig. 3(b)] is assigned to the N 2p_z orbital based on FP-LMTO and DFT calculations [24,30]. The feature at +4.0 V in the STS spectra [Fig. 3(b)] is dependent on the corrugation of the Cu_3N network where N_t atoms of the network do not clearly exhibit this electronic state. This feature at +4.0 V is appearing in the STS spectra only from the N_m and N_b atoms of the Cu_3N surface. We know that the actual adsorbate geometry in Cu_3N -Cu(110) involves a displacement of the surface Cu layer atoms from their original positions, and as a result N_t atoms are placed outward away from the N_m or N_b atoms giving rise to the corrugation present in the Cu_3N network [9]. This will cause a different N-Cu bond length with 1st and 2nd layer Cu atoms where possible contributions may come from other Cu orbitals [24]. Moreover, the enhanced N-Cu bond length of the N_t atoms will make σ bonds of the N 2p_z and the 2nd Cu layer even weaker [24]. Some mixing of the N 2p_{xy} and 2p_z orbitals might be possible in the σ and π bonds as well due to the corrugation in the system [24]. There is also a report on a weak surface state at

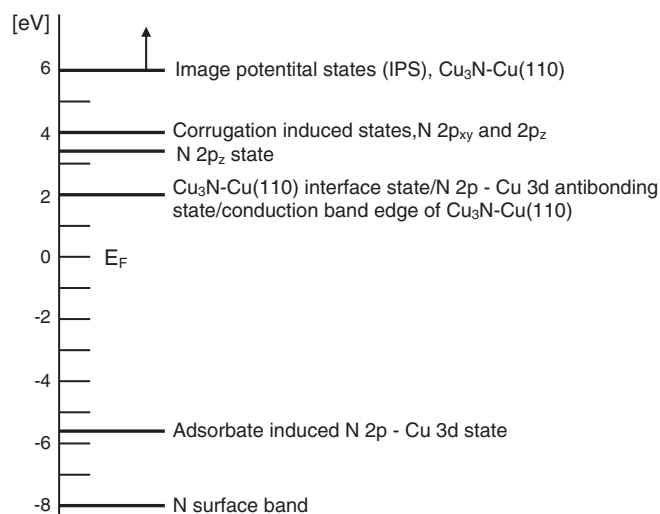


Fig. 6. Schematic energy level diagram showing various possible N 2p-Cu 3d hybridized states appearing from the STS measurements as discussed in the text.

4.0 eV above the Fermi level [28] as measured by inverse photoemission spectroscopy on clean Cu(110).

The peaks at +5.1 V and above [Fig. 3(b)] we assign to image potential states (IPS) [25,27,31], which are due to the screening of an extra charge in front of the metal surface by its conduction electrons. These hydrogen-like bound states that are confined along the surface normal and localized near the surface make them accessible by CC-STs. The energy position of the lowest image state is tied to the local work function of the material [32–36]. Resonant tunneling of electrons through these states gives step-like features in the $Z(V)$ spectra operating in the CC mode. The applied electric field within the tip-sample tunnel junction induces a stark shift of the states to higher energy values [25–31] such that the lowest resonance in the STS occurs at a bias slightly above the work function. Since the work function of Cu(110) is around 4.48 eV [37,38], the appearance of the 1st image state of the Cu(110) surface at +5.1 V for a tunneling current of 1 nA in our case [Fig. 3(d)] matches perfectly with the results of Dougherty et al. [31] who have also observed the occurrence of the 1st image state on Cu(110) at a similar position for the same tunneling current of 1 nA. A small shoulder-like feature is observed at approximately +4.6 V in the STS spectrum from clean Cu. This small feature is identified as the projected bulk band of Cu(110) [31]. The change in first image state is attributed to a change in the surface work function [39–42]. It has been reported [25] that CuN films on Cu(100) show an increase in the surface work function by 0.9 eV. In our case as well, a shift of the 1st image state by +0.9 V due to N adsorption is quite consistent with the prior study [25]. Calculations suggest that due to a substantial electronegativity difference between the adsorbed N atoms and the substrate Cu atoms ($3.04 - 1.90 = 1.14$), N atoms acquire a partial negative charge [23] and as a result there is a surface dipole moment present in the Cu_3N surface which would increase the surface work function consistent with the results presented here.

For the occupied electronic states [Fig. 4(b)], we attribute the features appearing at -4.9 V, -5.6 V in the STS spectra from bare Cu(110) to Cu 3d bands [24] and the feature at -7.4 V to Cu 4s band [43]. The peak at a similar position of -5.6 V from the Cu_3N surface is attributed to a primary adsorbate induced state derived from N 2p Cu 3d hybridization [24]. Previous photo and x-ray emission spectroscopy results on N adsorbed Cu(100) surface reveal electronic states at -1.3 eV and -5.5 eV related to nitrogen $2p_{xy}$ orbital that have hybridized with the Cu d band [24,44]. Though, we do not see any large significant onset at around -1.3 V in the CC-STs measurements, a change in differential conductivity is indeed observed clearly in the CH-STs studies [Fig. 2(b)]. The feature at -8.0 V originating from the Cu_3N surface might be due to a flat N-derived surface band which would appear around 7.5 eV below the Fermi level [24].

The SR-STs maps in Fig. 5(a, b) and the dI/dV profiles plotted in Fig. 5(c) help us further to verify the local electronic structure of the corrugated Cu_3N network. From the dI/dV profiles in Fig. 5(c), the period (λ) of the oscillations within the modulations at +2.0 V, +3.4 V and +4.0 V is estimated to be 1.13 nm, 1.145 nm and 1.13 nm, respectively, which correspond to an average periodicity of 1.135 nm along [001] [9]. These periodicities of 0.5 nm and 1.135 nm along [1–10] and [001] respectively correspond to the $p(2 \times 3)$ reconstructed unit cell of the N-terminated $\text{Cu}_3\text{N}-\text{Cu}(110)$ surface [9]. A phase shift of 180° is observed for the profile at +3.4 V with respect to the profiles at +2.0 V and +4.0 V. As we can see from Fig. 3(b), tunneling at +2.0 V and +4.0 V is dominated by N_m and N_b atoms, while tunneling at +3.4 V is dominated by N_t atoms of the Cu_3N surface. Thus, the signal at +2.0 V and +4.0 V oscillates with the periodicity of the N_m (and N_b) atoms, whereas at +3.4 V, the signal oscillates following the N_t atoms. Since, the N_t and N_m atoms are shifted by half of the unit cell [Fig. 1], the dI/dV curves corresponding to Fig. 3(b) are also shifted by half of the lattice constant along the [001] direction. The chemical nature of individual N (N_t , N_m or N_b)

atoms with the surface and subsurface Cu layers is rigorously verified by plotting such SR $dI(V, r)/dV$ maps.

5. Summary

In summary, we have shown that a combination of CH and CC STS measurements along with spatially resolved $dI(V, r)/dV$ maps is useful in providing a proper understanding of the local electronic properties of the corrugated $\text{Cu}_3\text{N}-\text{Cu}(110)$ network. Despite the fact that CH-STs measurements could probe the hybridized N–Cu antibonding states [23,24] around the Fermi level, CC-STs measurements were more useful in understanding the local electronic structure of the N terminated Cu(110) surface. Also, hybridized N 2p and Cu 3d states below the Fermi level were possible to be probed by CC STS measurements, where CH STS measurements showed only a huge tunnel current at a higher bias. The study of the 1st image potential states yields information about relative surface work function that is 0.9 eV higher for Cu_3N compared to clean Cu(110). This indicates that the charge density of the metal surface of Cu(110) is suppressed by the formation of a nitride layer. The surface corrugation responsible for different N–Cu bond lengths of N_t , N_m and N_b atoms with the surface and subsurface Cu layers plays a crucial role where the electronic structure of the $\text{Cu}_3\text{N}-\text{Cu}(110)$ surface varies locally as manifested in the atomically resolved STS studies.

Acknowledgement

We thank H. Menge for technical support.

References

- [1] J. Repp, G. Meyer, S.M. Stojković, A. Gourdon, C. Joachim, Phys. Rev. Lett. 94 (2005) 026803.
- [2] J. Repp, G. Meyer, Appl. Phys. A, Mater. Sci. Process 85 (2006) 399.
- [3] S. Schintke, S. Messerli, M. Pivetta, F. Patthey, L. Libioulle, M. Stengel, A. De Vitta, W.-D. Scheider, Phys. Rev. Lett. 87 (2001) 276801.
- [4] V.E. Henrich, Rep. Prog. Phys. 48 (1985) 1481.
- [5] T. Huang, J. Zhao, M. Feng, H. Petek, S. Yang, L. Dunsch, Phys. Rev. B 81 (2010) 085434.
- [6] F.M. Leibls, R. Davis, A.W. Robinson, Phys. Rev. B 47 (1993) 10052.
- [7] T.M. Parker, L.K. Wilson, N.G. Condon, F.M. Leibls, Phys. Rev. B 56 (1997) 6458.
- [8] C.F. Hirjibehedin, C.P. Lutz, A.J. Heinrich, Science 312 (2006) 1021; C.F. Hirjibehedin, C.-Y. Lin, A.F. Otte, M. Ternes, C.P. Lutz, B.A. Jones, A.J. Heinrich, Science 317 (2007) 1199.
- [9] X.-D. Ma, D.I. Bazhanov, O. Fruchart, F. Yildiz, T. Yokoyama, M. Przybylski, V.S. Stepanyuk, W. Hergert, J. Kirschner, Phys. Rev. Lett. 102 (2009) 205503.
- [10] H. Baek, S. Jeon, J. Seo, Y. Kuk, J. Korean Phys. Soc. 56 (2010) 620.
- [11] X.H. Qiu, G.V. Nazin, W. Ho, Science 299 (2003) 542.
- [12] J. Repp, G. Meyer, F.E. Olsson, M. Persson, Science 305 (2004) 493.
- [13] S.W. Wu, N. Ogawa, W. Ho, Science 312 (2006) 1362.
- [14] F.E. Olsson, P. Paavilainen, M. Persson, J. Repp, G. Meyer, Phys. Rev. Lett. 98 (2007) 176803.
- [15] M. Sterrer, T. Risse, U.M. Pozzoni, L. Giordano, M. Heyde, H.-P. Rust, G. Pacchioni, H.-J. Freund, Phys. Rev. Lett. 98 (2007) 096107.
- [16] L. Giordano, G. Pacchioni, J. Goniakowski, N. Nilus, E.D.L. Rienks, H.-J. Freund, Phys. Rev. Lett. 101 (2008) 026102.
- [17] J. Repp, G. Meyer, S. Paavilainen, F.E. Olsson, M. Persson, Science 312 (2006) 1196.
- [18] H. Ellmer, V. Repain, S. Rousset, B. Croset, M. Sotto, P. Zeppenfeld, Surf. Sci. 476 (2001) 95.
- [19] S.M. York, F.M. Leibls, Phys. Rev. B 64 (2001) 033411.
- [20] F.M. Leibls, Surf. Sci. 514 (2002) 33.
- [21] T.E. Wofford, S.M. York, F.M. Leibls, Surf. Sci. 522 (2003) 47.
- [22] T.E. Wofford, S.M. York, F.M. Leibls, Surf. Sci. 539 (2003) 186.
- [23] A. Soon, L. Wong, B. Delley, C. Stampfl, Phys. Rev. B 77 (2008) 125423.
- [24] T. Wiell, J.E. Klepeis, P. Bennich, O. Bjorneholm, N. Wassdahl, A. Nilsson, Phys. Rev. B 58 (1998) 1655.
- [25] C.D. Ruggiero, T. Choi, J.A. Gupta, Appl. Phys. Lett. 91 (2007) 253106.
- [26] R.S. Becker, J.A. Golovchenko, D.R. Hamann, B.S. Swartztruber, Phys. Rev. Lett. 55 (1985) 2032.
- [27] P. Wahl, M.A. Schneider, L. Diekhoener, R. Vogelgesang, K. Kern, Phys. Rev. Lett. 91 (2003) 106802.
- [28] B. Reihl, K.H. Frank, Phys. Rev. B 31 (1985) 8282.
- [29] D. Tang, C. Su, D. Heskett, Surf. Sci. 295 (1993) 427.
- [30] L. Triguero, L.G.M. Pettersson, Surf. Sci. 398 (1998) 70.
- [31] D.B. Dougherty, P. Maksymovych, J. Lee, M. Feng, H. Petek, J.T. Yates, Phys. Rev. B 76 (2007) 125428.
- [32] T. Jung, Y.W. Mo, F.J. Himpsel, Phys. Rev. Lett. 74 (1995) 1641.

- [33] N.V. Smith, Phys. Rev. B 32 (1985) 3549.
- [34] D. Straub, F.J. Himpsel, Phys. Rev. B 33 (1986) 2256.
- [35] P.M. Echenique, J.B. Pendry, Prog. Surf. Sci. 32 (1990) 111.
- [36] W. Steinmann, Th. Fauster, Laser Spectroscopy and Photochemistry on Metal Surfaces, in: H.-L. Dai, W. Ho (Eds.), World Scientific, Singapore, 1993.
- [37] P.O. Gartland, S. Berge, B.J. Slagsvold, Phys. Rev. Lett. 28 (1972) 738.
- [38] M.P. Marder, Condensed Matter Physics, 16, Wiley, New York, 2000, (Chap. 23).
- [39] S. Schintke, W.-D. Schneider, J. Phys. Condens. Matter 16 (2004) R49.
- [40] F.E. Olsson, M. Persson, J. Repp, G. Meyer, Phys. Rev. B 71 (2005) 075419.
- [41] D.B. Dougherty, P. Maksymovych, J. Lee, J.T. Yates Jr., Phys. Rev. Lett. 97 (2006) 236806.
- [42] D.C. Marinica, C. Ramseyer, A.G. Borisov, D. Teillet-Billy, J.P. Gauyacq, W. Berthold, P. Feulner, U. Hofer, Phys. Rev. Lett. 89 (2002) 046802.
- [43] R. Madhavan, J.L. Whitten, J. Chem. Phys. 77 (1982) 2673.
- [44] G.G. Tibbets, J.M. Burkstrand, J.C. Tracy, Phys. Rev. B 15 (1977) 3652.